Journal of Coastal Research	00	0	000–000	Coconut Creek, Florida	Month 0000

Coherence between Coastal and River Flooding along the California Coast

Kingsley O. Odigie* and Jonathan A. Warrick

United States Geological Survey
Santa Cruz, CA 95060, U.S.A.

www.cerf-jcr.org

www.JCRonline.org

ABSTRACT

Odigie, K.O. and Warrick, J.A., 0000. Coherence between coastal and river flooding along the California coast. *Journal of Coastal Research,* 00(0), 000–000. Coconut Creek (Florida), ISSN 0749-0208.

Water levels around river mouths are intrinsically determined by sea level and river discharge. If storm-associated coastal water-level anomalies coincide with extreme river discharge, landscapes near river mouths will be flooded by the hydrodynamic interactions of these two water masses. Unfortunately, the temporal relationships between ocean and river water masses are not well understood. The coherence between extreme river discharge and coastal water levels at six California river mouths across different climatic and geographic regions was examined. Data from river gauges, wave buoys, and tide gauges from 2007 to 2014 were integrated to investigate the relationships between extreme river discharge and coastal water levels near the mouths of the Eel, Russian, San Lorenzo, Ventura, Arroyo Trabuco, and San Diego rivers. Results indicate that mean and extreme coastal water levels during extreme river discharge are significantly higher compared with background conditions. Elevated coastal water levels result from the combination of nontidal residuals (NTRs) and wave setups. Mean and extreme (>99th percentile of observations) NTRs are 3–20 cm and ~30 cm higher during extreme river discharge conditions, respectively. Mean and extreme wave setups are up to 40 cm and ~20–90 cm higher during extreme river discharge than typical conditions, respectively. These water-level anomalies were generally greatest for the northern rivers and least for the southern rivers. Time-series comparisons suggest that increases in NTRs are largely coherent with extreme river discharge, owing to the low atmospheric pressure systems associated with storms. The potential flooding risks of the concurrent timing of these water masses are tempered by the mixed, semidiurnal tides of the region that have amplitudes of 2–2.5 m. In summary, flooding hazard assessments for floodplains near California river mouths for current or future conditions with sea-level rise should include the temporal coherence of fluvial and oceanic water levels.

ADDITIONAL INDEX WORDS: *Nontidal residual, wave setup, extreme river discharge*.

INTRODUCTION

The frequency and intensity of coastal flooding are influenced by global climate variability, weather patterns, sea levels, and the shape of the coastal landscape (Hallegatte *et al*., 2013; Hinkel *et al*., 2014; Milly *et al*., 2002; Sommerfield, Drake, and Wheatcroft, 2002). Flood-related coastal hazards are a concern for low-lying coastal regions, because a large part (greater than 1 billion) of the world's population lives within 100 km of a coastline at densities that are approximately three times the global mean (Dawson *et al*., 2009; Merkens *et al*., 2016; Neumann *et al*., 2015; Wong *et al*., 2014). In the United States, over 50% of the population lives in coastal counties and 23 of the 25 most densely populated counties in the nation are coastal (Arkema *et al*., 2013; Scavia *et al*., 2002). The human and financial cost of flood-related damage can be enormous (Hallegatte *et al*., 2013; Heberger *et al*., 2009; Kates *et al*., 2006). These flooding risks are expected to increase globally with climate change and associated sea-level rise (*e.g*., Hallegatte *et al*., 2013; Little *et al*., 2015).

Ocean waves and storm surges are important drivers of coastal flooding and morphological change, and as such they can pose hazards to coastal communities and infrastructure (Mawdsley and Haigh, 2016; Serafin and Ruggiero, 2014). Waves increase the mean water level and lead to discrete water-level maxima at the foreshore, referred to as wave setup and run-up, respectively (Stockdon *et al*., 2006). Energetic waves can produce run-up levels that are several meters higher than offshore water levels depending on the wave conditions and the shape and slope of the beach (*e.g*., Guza and Feddersen, 2012; Stockdon *et al*., 2006). Significant changes in wave heights, especially the extremes, have been reported and projected (*e.g*., Erikson *et al*., 2015; Young, Zieger, and Babanin, 2011) along the North American West Coast. These changes could have a greater impact than sea-level rise on coastal flooding and erosion in the U.S. Pacific Northwest (*e.g*., Ruggiero, 2013). In addition, flooding could be exacerbated by storm surge, which refers to a storm-induced elevated water level along the coast due to the low atmospheric pressure and onshore-directed winds associated with storm conditions (Kang, Ma, and Liu, 2016; Wahl *et al*., 2015). Therefore, improved understanding of the relationships among these water-level extremes (storm surges, waves, and extreme river discharge) will assist in the adaptation and possible mitigation of coastal flooding (Heberger *et al*., 2009).

The flooding of landscapes adjacent to river mouths is more complex than that along open coastal settings owing to the influence of both oceanic and fluvial processes (Wahl *et al*., 2015). Water-level fluctuations in and near river mouths are caused by combinations of ocean water levels, wave setup, river stage and discharge, and the hydraulic conditions of these

DOI: 10.2112/JCOASTRES-D-16-00226.1 received 8 December 2016; accepted in revision 4 June 2017; corrected proofs received 15 August 2017; published pre-print online XX Month XXXX.
*Corresponding author: kodigie@ucsc.edu

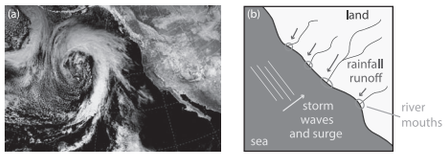

Figure 1. Conceptual framework for the coherence between coastal and extreme river discharge. (a) A typical winter storm in the North Pacific Ocean that will deliver precipitation, storm waves, and surge to the West Coast of North America as it travels eastward. (b) The effects of these storms converge at river mouths where coastal flooding from storm waves and surge meet river floods from rainfall runoff. Satellite imagery from NOAA GOES Geocolor obtained 22 February 2016 at 2100 UTC.

coastal river mouths (Guza and Feddersen, 2012; Ruggiero *et al*., 2001; Stockdon *et al*., 2006). The near-simultaneous arrival of large waves, storm surge, and high river discharge can magnify flooding adjacent to river mouths along coasts such as in California (Figure 1; Cayan *et al*., 2008; Guillén *et al*., 2006). In addition, seasonal elevation of water levels resulting from semiregular climate events (*e.g*., due to steric effects and coastally trapped waves, including during El Niño along the Pacific Coast) could add up to ~30 cm to coastal water level (Enfield and Allen, 1980). Unfortunately, information on the spatial and temporal relationships among extreme river discharge, storm surge, and wave setup is limited, so the potential effects of these combined processes on coastal flooding is unknown.

The objective of this study is to investigate the temporal and spatial relationships between river and coastal flooding across a range of geographic and climatic zones of coastal California (Figure 2). California has an extensive coastline of more than 3200 km that includes rocky shorelines, beaches, embayments, and wetlands. Additionally, over 80% of the state's population lives in coastal counties, which highlights the threat that coastal flooding poses to infrastructure, coastal habitats, and human lives in low-lying regions (Arkema *et al*., 2013; Crossett *et al*., 2004; Heberger *et al*., 2009; National Research Council, 2012; U.S. Census Bureau).

A primary goal of this work was to assess the temporal coherence of extreme river discharge conditions and elevated coastal water levels (*e.g*., nontidal residuals [NTRs] and waves) across a range of sites. Previous analyses suggest that storm conditions that deliver fine-grained sediment to the California coast and transport this sediment on the continental shelf are generally coherent in time owing to the large frontal storms originating over the North Pacific Ocean that generate rainfall and waves (Figure 1a; Kniskern *et al*., 2011). This paper seeks to extend this understanding of storm coherence to the topic of coastal flooding. These analyses are based on a synthesis of available ocean and river monitoring data for the California study area.

METHODS

A series of river mouth sites along the California coast were chosen on the basis of the availability and quality of coincidental coastal and river monitoring data. The focus of the analysis was to assess whether elevated coastal water

Figure 2. Map of California showing river gauges, buoys, and tide gauges at the study sites.

levels (NTRs and wave setup) occurred coincidentally in time with extreme river discharge, which might increase the risk of flooding in river mouth regions. Coastal flooding can occur during times with low river flow, *i.e*., "dry" times, and with large ocean swell generated from distant storms that do not make landfall on the watersheds of interest, and this contrasts with storms that cause precipitation over the watersheds (Guillén *et al*., 2006; Kniskern *et al*., 2011). The occurrence and influence of wet storms were assessed with comparisons of oceanic conditions both with and without high river flow. A detailed description of the methods follows.

Study Sites

California is the most populous state in the United States, with a population of approximately 38.8 million people in 2014 (U.S. Census Bureau). It has a temperate, Mediterranean climate, with greatest precipitation in the winter season; precipitation varies geographically, with the highest amounts in the north (CA DWR, 2003). Eastward-propagating storms originating over the North Pacific Ocean (Figure 1a) are responsible for the highest amounts of precipitation, the largest waves, and low atmospheric pressures that, combined, result in elevated water levels along the coast (Kniskern *et al*., 2011; Storlazzi and Griggs, 2000; Storlazzi, Willis, and Griggs, 2000). These coastal flooding conditions can be exacerbated by El Niño conditions, when winter storms and wave conditions are more extreme and sea levels across the region are seasonally elevated because of steric effects and the northward propagation of coastally trapped waves (Allan and Komar, 2002; Barnard *et al*., 2015). Additionally, the highest tides of the year typically occur during the winter, and if they coincide with these storms – as they did in Southern California during the winter of 1983, some of the strongest events ever recorded –

Table 1. *Stations and available stage, wave, and tide data for the different river systems studied.*

River System	Drainage Basin (km^2)	Flow Distance to Pacific Ocean (km)	USGS River Station (dates)	NOAA Wave Buoy (dates)	NOAA Coastal Water Levels (dates)
Eel	~8300[†]	~250[†]	11477000 (1 October 2007–15 March 2016)	46022 (1982–2015)	9418767 (1977–2015)
Russian	~3800[‡]	~177[§]	11467002 (19 December 2007–15 March 2016)	46013 (1981–2015)	9415020 (1973–2015)
San Lorenzo	~357[‖¶]	~47[‖¶]	11161000 (1 October 2007–15 March 2016)	46236 (2007–15)	9413450 (1973–2015)
Ventura	~590[#]	~54[#]	11118500 (1 October 2007–15 March 2016)	46217 (2004–15)*	9411340 (1979–80; 1990–98; 2005–15)
Arroyo Trabuco	~140[††]	~39[††]	11047300 (1 October 2007–15 March 2016)	46223 (2004–15)*	9410660 (1923–2016)
San Diego	~1140[‡‡]	~72[§§]	11023000 (1 October 2007–15 March 2016)	46231 (2005–15)*	9410230 (1924–47; 1948; 1949–54; 1955–71; 1972–2015)

**Additional (earlier) data might be available at http://cdip.ucsd.edu/.*
[†]*Sloan, Miller, and Lancaster (2001).*
[‡]*Christian-Smith and Merenlender (2010)*
[§]*Flint and Flint (2012)*
[‖]*Griggs and Paris (1982)*
[¶]*Conaway* et al. *(2013)*
[#]*Walter (2015)*
[††]*McVan (1997)*
[‡‡]*Bernstein (2014)*
[§§]*California Water Resources Control Board (2008).*

flooding can be exacerbated (Flick, 2016; Flick and Cayan, 1984; Moore, Benumof, and Griggs, 1999).

This study focuses on six river settings that have adequate wave, tidal, and river monitoring data to evaluate extreme river discharge and coastal water-level coherence patterns over several years, and thus, dozens of storms. These rivers are the Eel, Russian, San Lorenzo, Ventura, Arroyo Trabuco, and San Diego (Figure 2; Table 1). These rivers originate in the coastal ranges and discharge directly to the ocean, which contrasts with the larger Sacramento and San Joaquin river systems of California's Central Valley that are dominated by snowmelt hydrology from the Sierra Nevada and discharge into the largest inland estuary of the state, the San Francisco Bay estuary (Farnsworth and Warrick, 2007; Willis and Griggs, 2003). The sizes of the drainage basins and distances between the headwaters of these rivers and the Pacific Ocean are summarized in Table 1.

Data Sources

Three primary data sources were used for this study: river data from U.S. Geological Survey (USGS) gauging stations, ocean wave data from National Oceanic and Atmospheric Administration (NOAA) buoy stations, and predicted and measured coastal water levels from NOAA tidal stations. To evaluate coherence among these data, intervals in time were needed for which all measurements overlapped. A summary of the available data for the sites reveals that coincidental intervals of time included 2007 to 2014 (Table 1).

For each river site, channel and flow data for the most seaward gauging station in the watershed were obtained from USGS National Water Information System (NWIS) database (USGS). River water stage (water level above a reference elevation) data at 15-minute intervals were obtained for the six rivers (Table 1, Figure 2). These data were generally limited to 2007 to 2014. Additionally, river discharge and channel geometry data were obtained for each station to evaluate flood routing timing from the USGS station to the coast.

Wave data (*i.e.* significant wave height, peak period, and peak direction) were obtained from the NOAA Buoy database (NOAA [a]) for the stations closest to the six river mouths (Table 1, Figure 2). Sampling intervals for the wave data generally ranged from 15 minutes to an hour, with some missing data. Wave data were generally available from 1980s to present (Table 1).

Hourly predicted and observed water levels were obtained from the NOAA Tide and Currents database (NOAA [b]) for stations nearest to the river mouths (Table 1, Figure 2). These stations are in harbors and embayments and have data starting from the 1920s to present (Table 1).

River Stage

Because the USGS river gauging stations were located several kilometers upstream of the coast, the timing of the high flows had to be offset to account for delays in river flood travel times between the gauges and the ocean. Flood routing principles were used to estimate travel times of river discharge peaks from the gauging stations to the coast. Using the advection–diffusion analogy for flood wave propagation, the kinematic wave speeds were estimated from the slopes between channel area and river discharge for each gauging station (Bras, 1990). Field measurements of river discharge and channel properties were obtained from the USGS NWIS database, and linear relationships between channel area and discharge were computed with linear regression (*e.g.*, Figure S4). The data sets ranged between 365 and 1006 measurements and their coefficients of determination (r^2) ranged between 0.87 and 0.96, with a mean of 0.91. Resulting estimates of the kinematic wave speed ranged between 1.1 and 2.8 m s^{-1}, and these speeds resulted in flood wave travel times that varied between 0.5 and 4.6 hours from the stations to the coast (Table 2). These analyses assume that the channels at the gauges

Table 2. *Estimated travel times of river flood waves from gauging stations to the coast and approximate sizes of drainage areas incorporated by the gauges*.

River System	Estimated Kinematic Wave Speed (m/s)	Distance from Gauge to Coast (km)	Travel Time of River Flood Wave (h)	Gauge Drainage Area (km^2)
Eel River	2.8	31.7	3.1	8063
Russian River	1.5	24.6	4.6	3504
San Lorenzo River	1.4	3.99	0.8	297.8
Ventura River	2.5	9.70	1.1	486.9
Arroyo Trabuco	2.4	4.73	0.5	140.1
San Diego River	1.1	8.26	2.1	1111

were representative of the remaining channels between the gauges and the coast, and thus are assumed to be first-order estimates of the travel times. Estimated travel times were used to delay the river stage measurements for all computations and analyses.

Waves and Wave Setup

Wave setup was used to estimate the effects of ocean waves on river mouth flooding. Although wave run-up over beach berms adjacent to the river mouth may contribute ocean water to the river mouth and thus exacerbate flooding, wave setup would more likely control the hydraulic pressure gradients at the river mouth inlet and thus provide a more dominant effect on river mouth flooding.

The wave data were used to estimate wave setup adjacent to river mouths by using: (1) linear wave theory to transfer storm waves from the buoys to the shoreline and (2) standard empirical procedures to estimate wave setup. The lags between the wave measurement times at the buoys and times for the waves to reach the shoreline were estimated using linear wave theory as shown in Equations (1) and (2) below (Bowden, 1983; Knauss, 1978):

$$C_g = \frac{1}{2}\frac{gT}{2\pi} \tag{1}$$

$$t = \frac{d}{C_g}\cos\theta \tag{2}$$

where, C_g is the group velocity (m s^{-1}) of wave, g is acceleration due to gravity (9.8 m s^{-2}), T is the dominant wave period (s), t is the estimated time (s) for the wave to travel from the buoy to the river mouth, d is the distance (m) between the buoy and river mouth, and θ is the difference between direction of river mouth from the buoy and angular deviation of wave travel from perpendicular to the shoreline.

The wave lags (t) were computed for available buoy data with significant wave height, dominant wave period, and dominant wave direction data and these values averaged between –2 and 0.9 minutes for the six sites, with a pooled mean of ~0 minutes. Unfortunately, more than 50% of the wave data for two sites were missing direction records, which limited the potential for estimating these values. Consequently, no adjustments were made to the times for the waves to reach the river mouths from the buoys, *i.e.* mean zero lags were adopted for all river systems.

Wave setup ($<\eta>$) was computed using the methods described by Stockdon *et al*. (2006):

$$L_0 = \frac{gT^2}{2\pi} \tag{3}$$

$$<\eta> = 0.35\beta_f(H_0L_0)^{1/2} \tag{4}$$

where, L_0 is the deepwater wavelength (m), g is acceleration due to gravity (9.8 m s^{-2}), T is the dominant wave period (s), and β_f is beach slope. A range of beach slopes (β_f) from 0.01 to 0.1 was used for each site to incorporate the potential variability in beach morphology near the river mouth sites. However, the primary effect of β_f was on the relative magnitude of wave setup; β_f had negligible effect on the temporal patterns of coastal flooding. Thus, for the results presented here, all results are shown for β_f values of 0.1.

Tides and NTRs

NTR, which is a measure of the water-level difference from the predicted tide, was computed to assess storm surge and seasonal water-level anomaly contributions during extreme river discharge conditions. Since the tidal gauge stations are located at harbors or embayments, no lag correction was necessary. NTR (m) was computed by subtracting the predicted tide from the observed water level for each record:

$$\text{NTR (m)} = \text{observed water level (m)} - \text{predicted tide (m)} \tag{5}$$

Coherence Analyses

Two primary analyses were used to evaluate flooding coherence across rivers and coastal waters during the study periods. First, an overarching assessment was made to evaluate whether the distributions of wave setup and NTR during extreme river discharge were different from those at other intervals of time. For this assessment, the "flooding stage" was defined for each river as gauge heights greater than the 99th percentile of all stage records. Then, wave setup and NTR records for intervals of time that the rivers exceeded the extreme river discharge stages were selected and compared with wave setup and NTR records for the entire study period. For these comparisons, distributions were compared and student's t test of the means were made.

Second, an evaluation of the temporal coherence during storms was conducted with the master time series. For this evaluation, extreme river stages were defined by river stages that exceeded the 99th percentile of all stage records for the study period as previously defined. The peaks of continuous extreme stage (>99th percentile stage) events were identified, and an interval of ±4 days about each peak time was used to extract data to define conditions before and after an event (*cf*. Kniskern *et al*., 2011; Figure 3). The events (including the peaks and ±4 days) were selected such that there were no overlaps between adjacent events. Then the stage, NTR, and wave setup data for each event were converted to hours relative to the peak stage time (0 h) for each extreme event. Where minor gaps (≤5 h) in the wave and tide data existed, values were estimated using the piecewise cubic hermite interpolating polynomial (PCHIP), a shape-preserving interpolation algo-

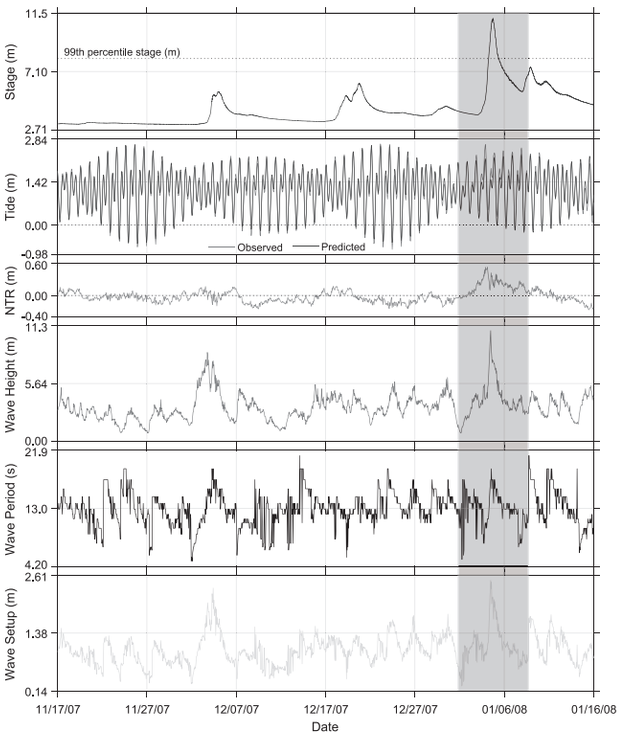

Figure 3. Time series of stage, tidal water levels (observed, predicted, and nontidal residual), and wave (height, period, and setup) data from Eel River in California. The shaded area represents a typical extreme river discharge event time series (peak stage ± 4 d).

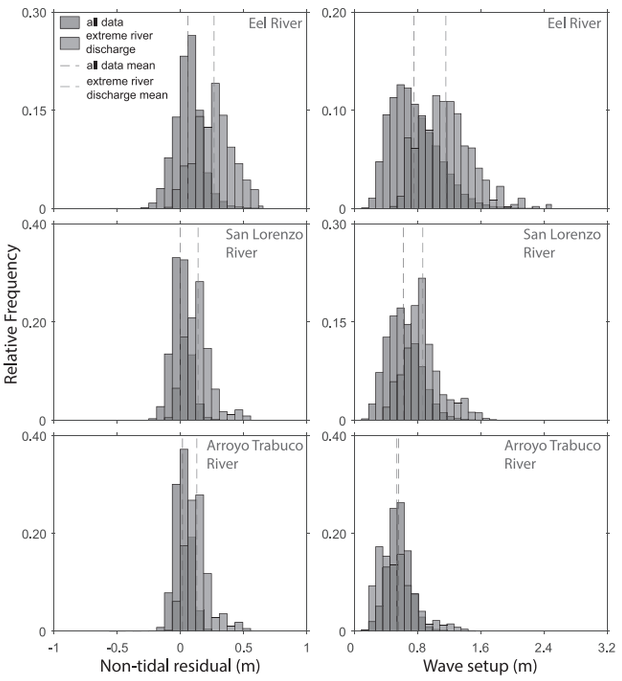

Figure 4. Histograms showing distributions of nontidal residual and wave setup data during extreme river discharge events and entire study periods for Eel, San Lorenzo, and Arroyo Trabuco rivers in California.

rithm, in MATLAB (The MathWorks, 2016). The time series of river stage, NTR, and wave setup were resampled at 30-minute intervals using the PCHIP for synchrony because the original data were collected at different intervals. The resampled data were consistent with the original data (see Supplementary Materials, Figures S1 to S3). For each study site, the events were combined using the time of peak stage as reference (set to 0 h), and percentiles were computed for the stage, wave setup, and NTR records.

RESULTS

An example time-series plot showing stage, predicted and observed water levels, NTR, wave height and period, and wave setup data from the Eel River stations over a period of 2 months is presented in Figure 3. Three intervals of elevated river stage are observed in this time series (early December, mid-December, and early January), and these river events generally coincided with elevated ocean water levels from wave setup and NTR. The final river event presented in Figure 3 surpassed the 99th percentile of recorded river stages, and was defined, therefore, as a single flooding event for the purpose of this paper. This event coincided with tens of centimeters of NTR, offshore wave heights in excess of 9 m, and computed wave setup in excess of 2 m (Figure 3).

A comparison between the distributions of wave setup and NTR for the entire record and for intervals of time of extreme river discharge is presented in Figure 4 for three of the six study sites – Eel, San Lorenzo, and Arroyo Trabuco rivers. Identical histograms for the three remaining study sites are presented in the Supplementary Materials as Figure S5. NTR and wave setup are generally higher during extreme river discharge conditions for all river systems. One exception is wave setup conditions for the Arroyo Trabuco system, which had slightly lower mean values during extreme river discharge (Figure 4; upper panel Figure 5). Student's t tests for comparisons of the NTR and wave setup means were highly significant ($p < 0.001$) for all sites except wave setup for the Arroyo Trabuco (Table 3).

The extreme values of NTR and wave setup during extreme river discharge were notably larger for all study sites as shown by the distributions of the observations (Figure 5). Using the 99th percentile of the observations as a metric for these extreme values, all study sites are shown to have greater extreme NTR and wave setup during extreme river discharge than during typical conditions (lower panel, Figure 5). Extreme NTR was 11–36 cm greater during extreme river discharge than typically observed. Similarly, extreme wave setup was 18–93 cm higher during extreme river discharge (Figure 5). These observations were similar to the mean values, which revealed that NTR and wave setup values were greatest in the northern region of California, and that the differences between storm surge during extreme river discharge and typical conditions were generally greatest in the northern study sites (Figure 5).

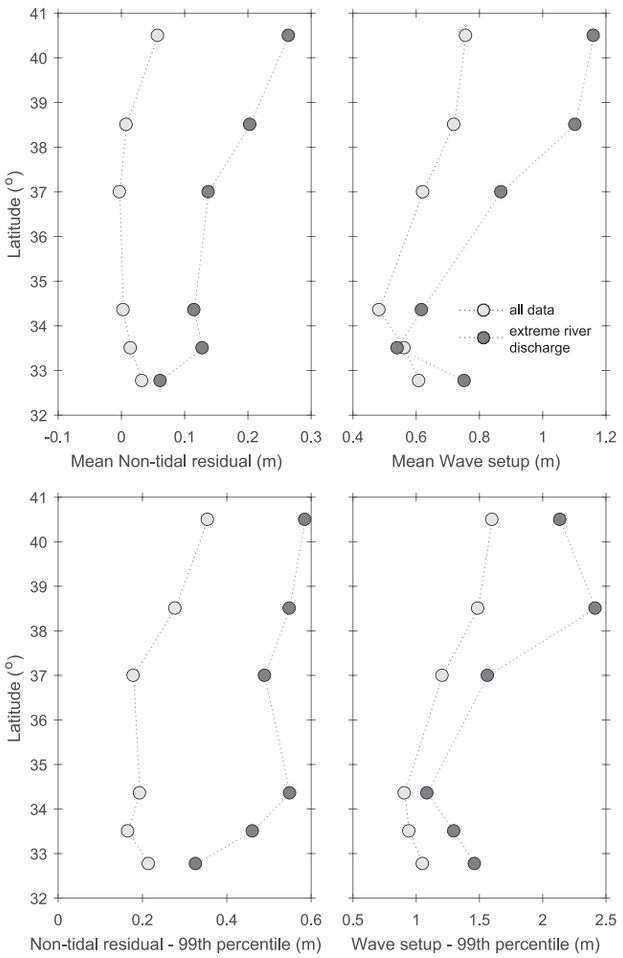

Figure 5. Variations of the mean and 99th percentile nontidal residual (m) and wave setup (m) with latitude along the coast of California.

The coherence of storm surges and waves during extreme river discharge events can be further assessed by the aggregated time series of river stage, NTR, and wave setup during extreme river discharge events (Figures 6–8). Similar aggregated plots for the Russian, Ventura, and San Diego rivers are presented in the Supplementary Materials as

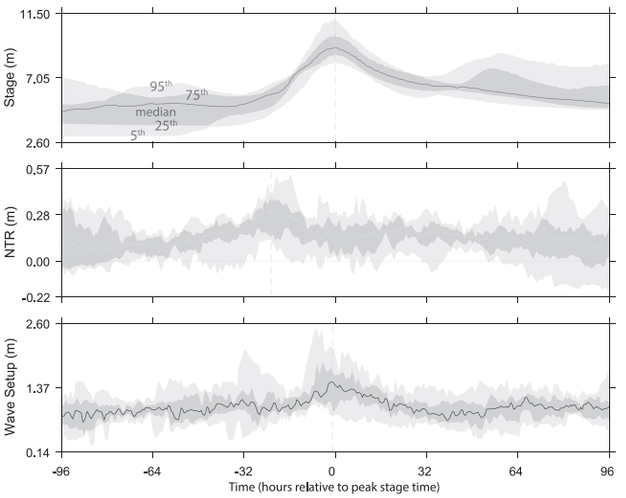

Figure 6. Time-series plots of aggregated (n = 8) Eel River stage (m), nontidal residual (m), and wave setup (m) events data. The annotations are the computed percentiles. Vertical dashed lines mark the median peaks of the plots.

Figures S6–S8. In general, the time-series data reveal that substantial variability exists in the NTR and wave setup data, and that both NTR and wave setup exhibit coherent patterns with extreme river discharge, although not always synchronous. For example, median NTR for the Eel River system appears to peak at 20–30 hours before median peak river discharge, whereas the median peak of wave setup is in phase with river discharge (Figure 6). In contrast, NTR for the San Lorenzo and Arroyo Trabuco systems – although less pronounced than the Eel River system – are in phase with river discharge (Figures 7 and 8). Wave setup for the San Lorenzo and Arroyo Trabuco systems reveal highly variable phasing with peak river discharge (Figures 7 and 8).

DISCUSSION

The flooding response of a coastal region to the combined effects of NTR, wave setup, and extreme river discharge will be a complex interaction of the hydrologic water balance, hydrodynamic forcings, the physical geometry of the flooding and surrounding areas, and potential morphodynamic change (erosion and deposition) that may be caused by the flows of

Table 3. *Comparisons of river stage, nontidal residual, and wave setup results for each river study site.*

River Study Site	River Stage (m)			Nontidal Residual (m)			Wave Setup (m)		
	Range (all)	Median (all)	99th (all)	Mean (all)	Mean (extreme river discharge)	99th (all)	Mean (all)	Mean (extreme river discharge)	99th (all)
Eel	2.6–14	3.3	8.1	0.06	0.26**	0.36	0.76	1.2**	1.6
Russian	1.7–9.3	2.5	7.4	0.008	0.20**	0.28	0.72	1.1**	1.5
San Lorenzo	1.0–6.8	1.7	2.9	—0.002	0.14**	0.18	0.62	0.87**	1.2
Ventura	0.2–5.3	1.8	2.2	0.003	0.12**	0.19	0.48	0.62**	0.91
Arroyo Trabuco	3.2–5.8	3.3	3.6	0.015	0.13**	0.17	0.56	0.54 n.s.	0.95
San Diego	0.5–4.3	0.6	1.7	0.03	0.06**	0.22	0.61	0.75**	1.1

**p $<$ *0.001, statistical significance of student's t test comparison of means*
n.s., not significant at p $>$ *0.05.*

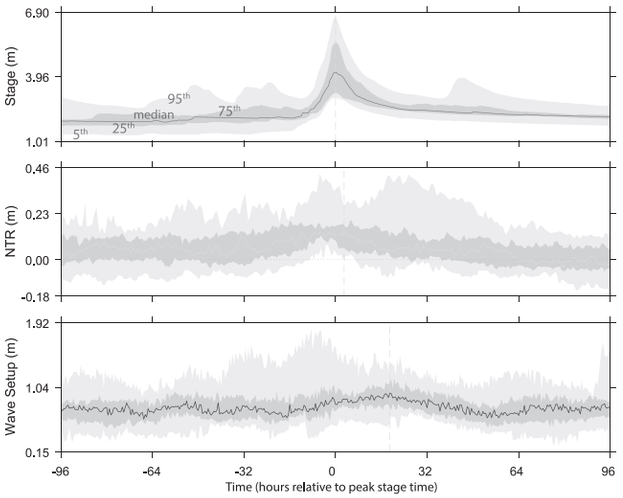

Figure 7. Time-series plots of aggregated ($n = 17$) San Lorenzo River stage (m), nontidal residual (m), and wave setup (m) data. The annotations are the computed percentiles. Vertical dashed lines mark the median peaks of the plots.

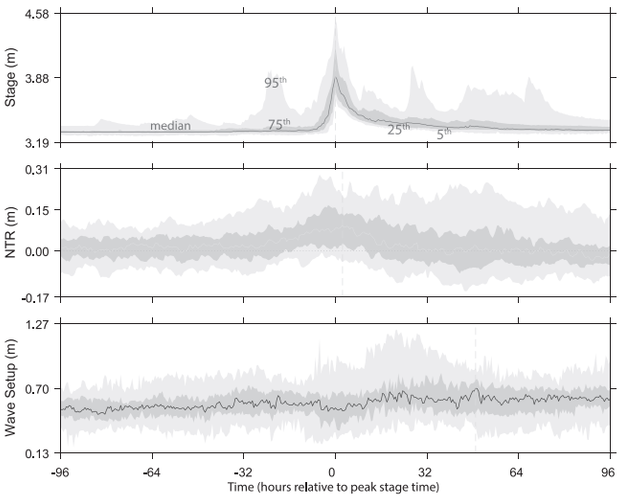

Figure 8. Time-series plots of aggregated ($n = 24$) Arroyo Trabuco River stage (m), nontidal residual (m), and wave setup (m) data. The annotations are the computed percentiles. Vertical dashed lines mark the median peaks of the plots.

water. For example, coastal flooding in river mouths can be influenced by inputs of water from wave setup overtopping the beach berm (Schwarz and Orme, 2005), and this additional input of water can cause breaching and erosion of the beach berm, which could further influence the hydrodynamics of the river mouth region. These kinds of dynamics are prevalent for the coastal river mouths of California, including the study sites, owing to the propensity of these systems to partially or fully close along the littoral interface (Jacobs, Stein, and Longcore, 2010).

The oceanic conditions that cause coastal flooding – NTR and wave setup – were on average elevated during extreme river discharge along the coastal watersheds of California (Figure 5). Additionally, the results show that the NTR and wave setup levels varied latitudinally – both during extreme river discharge conditions and for the entire study period (Figure 5). The variations are, at least partly, due to wave exposure to Pacific swell, which are greatest in the north and least in the south (*cf.* Adams, Imnan, and Graham, 2008) and the location of the North Pacific low during the winter storm season (*cf.* Bromirski, Flick, and Cayan, 2003). The disparities in NTRs and wave setups across the different latitudes can be considered coastal "microclimatic" conditions that characterize the river basins and their propensity to flood. It is notable that the northernmost river basins (Eel and Russian rivers) have the largest wave setup and NTR effects and also have the largest amounts of precipitation (CA DWR, 2003).

It is important to assess both the causes and implications of these coherence conditions. Floods in California are most commonly caused by intense precipitation related to low-pressure atmospheric systems that develop over the northern Pacific Ocean and incorporate moist subtropical air masses in "atmospheric rivers" (Ralph *et al.*, 2006). These low-pressure systems are also responsible for elevated wind speeds over broad swaths of the northern Pacific Ocean, which result in the large waves (*e.g.*, Ruggiero, 2013). In this manner, it should be expected that flooding conditions in the coastal river systems would occur coincidentally with the coastal flooding conditions produced by storm waves and elevated water levels (*cf.* Kniskern *et al.*, 2011). Additionally, these findings are consistent with the longer-term assessments of NTR, which suggest that elevated water levels are related to intense storms from southerly displaced "Aleutian low" atmospheric pressure systems that cause more frequent and more intense storms for the California coast (Bromirski, Flick, and Cayan, 2003).

It is also important to assess what contributes to the elevated NTR water levels measured at the tidal gauges during extreme river discharge. These water levels will be influenced by several factors, including displacement from freshwater input (Warrick *et al.*, 2004), elevated water levels from warm water masses during El Niño conditions (Flick, 1998; Storlazzi, Willis, and Griggs, 2000), and the "inverse barometric pressure" effect on water levels (Bromirski, Flick, and Cayan, 2003). The upward displacement of the ocean water surface from buoyant freshwater input is likely minimal; for example, the maximum displacement of 1.1 cm was computed by Warrick *et al.* (2004) immediately offshore of a Southern California river during flood stage. El Niño, in contrast, can result in tens of centimeters of elevated sea level during the winter season, and El Niño winters generally have the greatest rainfall and highest wave heights (Flick, 1998; Storlazzi, Willis, and Griggs, 2000). Last, the sea-level pressure along California can drop by over 20 mbar during winter storms, and although the expected water-level response related to this pressure decrease is $\sim$1 cm mbar^{-1}, Bromirski, Flick, and Cayan (2003) note that water levels can rise up to 1.65 cm mbar^{-1} along the California coast.

The implications of these elevated water levels are that flooding hazards around the region's river mouths are not simply related to the independent effects of coastal and river water levels. Rather, flooding in the river mouths of California is related to dependent relationships and temporal coherence between river and coastal conditions. Combined, these coherent conditions will regularly add tens of centimeters to coastal water levels (Figures 3–5) and occasionally add a meter or more.

The flooding risks associated with these coherent conditions will largely be dependent on tidal stage during the events, which can vary by several meters (*e.g.*, Figure 3). In fact, the most notable coastal flooding in California has been documented when peak extreme river discharge and wave heights occurred coherently with high spring tides (Flick, 1998; Griggs and Paris, 1982; Storlazzi, Willis, and Griggs, 2000).

Although flooding has been documented in and around several California river mouths, the effects of the combination of river and coastal flooding has not been investigated. For example, catastrophic floods from big storms and subsequent overflow of the Eel River have been documented, including in 1955 and 1964 when floods resulted in severe damages to buildings and vegetation in the river's basin and flooding throughout the lower watershed (Brown and Ritter, 1971; Sloan, Miller, and Lancaster, 2001). Similarly, the Russian and San Lorenzo rivers are noted to be flood prone, and several incidents of storm-related floods have been documented in their basins (*e.g.*, Griggs and Paris, 1982; Ralph *et al.*, 2006). What is not known – and deserves more attention – is how much of the historic flooding in the lower watersheds was influenced by elevated water levels along the coast, which may have flooded the river mouth regions before, during, or after the river discharge events or inhibited the outflow of riverine water to the sea. That is, how much of historic flooding in the lower watersheds was related to the combined and coherent nature of coastal and riverine conditions?

These questions are especially important in evaluating the future impacts of elevated coastal water-level events and episodic river discharge because of future sea-level rise (Cayan *et al.*, 2008; Rahmstorf, 2007). The superimposition of present day storm-driven coastal water-level anomalies and episodic river discharge with projected sea levels could increase the threat to many coastal regions, and possibly render some coastal areas uninhabitable (Bjerklie *et al.*, 2012; Cayan *et al.*, 2008; Rahmstorf, 2007; Rotzoll and Fletcher, 2013). The availability of more data sets and hydrodynamic models could help us to understand the interactions among these water masses better. Additionally, it is noteworthy that the actual risks – to humans and infrastructure – from flooding near river mouths will depend on the level of development and population near these landforms. For example, the Eel and Russian rivers drain the wettest and largest basins among the study sites, but their mouths are in relatively rural/unpopulated areas, which contrasts with the mouths of the San Lorenzo and San Diego rivers, which are in urban areas (Table 1; OSHPD; Griggs and Paris, 1982).

CONCLUSIONS

Previous studies have attributed damages, loss of lives, displacement of people, and coastal ecosystem impacts to floods caused by river overflow (*e.g.*, Griggs and Paris, 1982). Similarly, damages attributable to coastal storms, including hurricanes, can run into billions of dollars (Kates *et al.*, 2006). Here the potential for flooding conditions in rivers and coastal waters to coincide in time was investigated for the small watersheds of California. If the arrival times for these flooding conditions overlap, then the flooding hazard for these river mouths will be related to the combination – and interrelation – of these physical processes.

The results of this study demonstrate the relative concurrent occurrence of coastal water-level anomalies (*e.g.*, NTR and wave setup) and extreme river discharge along the California coast. The results also show that NTR and wave setup during extreme river discharge events are related to latitude, with the greatest values occurring in the northernmost river systems. These results have important implications, especially with the consideration of predicted changes in sea level and rainfall patterns in response to global climate change (Cayan *et al.*, 2008; IPCC, 2013; Rahmstorf, 2007). Consequently, improved understanding of the relationship between coastal water levels and river discharge will be important in protecting humans, ecosystems, and infrastructure in coastal regions. Future coastal hazards assessments for California and other regions with similar coherence between river and ocean systems would benefit from incorporating the combination of coastal water levels, episodic riverine discharge, and different scenarios of sea-level rise to adequately map flooding hazards.

ACKNOWLEDGMENTS

The authors thank Dr. Peter W. Swarzenski and Prof. A. Russell Flegal for their support during this project. The authors appreciate Dr. Patrick Barnard, Dr. Li Erikson, and four anonymous reviewers for their constructive comments that substantially improved the manuscript. The opinions expressed in this manuscript are those of the authors and do not represent the view of the U.S. Government. The use of trade names does not indicate endorsement by the U.S. Government.

LITERATURE CITED

Adams, P.N.; Imnan, D.L., and Graham, N.E., 2008. Southern California deep-water wave climate: Characterization and application to coastal processes. *Journal of Coastal Research,* 24(4), 1022–1035. doi:10.2112/07-0831.1

Allan, J.C. and Komar, P.D., 2002. Extreme storms on the Pacific Northwest coast during the 1997–98 El Niño and 1998–99 La Niña. *Journal of Coastal Research,* 18(1), 175–193.

Arkema, K.K.; Guannel, G.; Verutes, G.; Wood, S.A.; Guerry, A.; Ruckelshaus, M.; Kareiva, P.; Lacayo, M., and Silver, J.M., 2013. Coastal habitats shield people and property from sea-level rise and storms. *Nature Climate Change,* 3(10), 913–918. doi:10.1038/Nclimate1944

Barnard, P.L.; Short, A.D.; Harley, M.D.; Splinter, K.D.; Vitousek, S.; Turner, I.L.; Allan, J.; Banno, M.; Bryan, K.R., and Doria, A., 2015. Coastal vulnerability across the Pacific dominated by El Niño/Southern Oscillation. *Nature Geoscience,* 8(10), 801–807.

Bernstein, B.B., 2014. *San Diego River Watershed Monitoring and Assessment Program*. San Diego Regional Water Quality Control Board, *Report SWAMP-MR-RB9-2014-0001*, 95p.

Bjerklie, D.M.; Mullaney, J.R.; Stone, J.R.; Skinner, B.J., and Ramlow, M.A., 2012. *Preliminary Investigation of the Effects of Sea-Level Rise on Groundwater Levels in New Haven, Connecticut*. U.S. Geological Survey, *Open-File Report 2012–1025*, 46p.

Bowden, K.F., 1983. *Physical Oceanography of Coastal Waters*. Chichester, U.K.: Ellis Horwood, 302p.

Bras, R.F., 1990. *Hydrology: An Introduction to Hydrologic Science*. Reading, Massachusetts: Addison-Wesley, 643p.

Bromirski, P.D.; Flick, R.E., and Cayan, D.R., 2003. Storminess variability along the California coast: 1858–2000. *Journal of Climate,* 16(6), 982–993. doi:10.1175/1520-0442(2003)016<0982:Svatcc>2.0.Co;2

Brown, W.M., III, and Ritter, J.R., 1971. *Sediment Transport and Turbidity in the Eel River Basin, California*. U.S. Government Printing Office, *Geological Survey Water-Supply Paper 1986*, 67p.

CA DWR (California Department of Water Resources), 2003. *California's Groundwater*. Califoria Department of Water Resources. http://www.water.ca.gov/pubs/groundwater/bulletin_118/california's_groundwater__bulletin_118_-_update_2003_/bulletin118_entire.pdf.

California Water Resources Control Board, 2008. *Restoration of a Reach of the San Diego River within the Unincorporated Community of Lakeside, San Diego County, California*. http://www.waterboards.ca.gov/water_issues/programs/nps/docs/success/r9_lakeside.pdf.

Cayan, D.R.; Bromirski, P.D.; Hayhoe, K.; Tyree, M.; Dettinger, M.D., and Flick, R.E., 2008. Climate change projections of sea level extremes along the California coast. *Climatic Change,* 87, S57–S73. doi:10.1007/s10584-007-9376-7

Christian-Smith, J. and Merenlender, A.M., 2010. The disconnect between restoration goals and practices: A case study of watershed restoration in the Russian River Basin, California. *Restoration Ecology,* 18(1), 95–102. doi:10.1111/j.1526-100X. 2008.00428.x

Conaway, C.; Draut, A.; Echols, K.; Storlazzi, C., and Ritchie, A., 2013. Episodic suspended sediment transport and elevated polycyclic aromatic hydrocarbon concentrations in a small, mountainous river in coastal California. *River Research and Applications,* 29(7), 919–932.

Crossett, K.M.; Culliton, T.J.; Wiley, P.C., and Goodspeed, T.R. 2004. *Population Trends along the Coastal United States: 1980–2008: Coastal Trends Report Series*, National Oceanic and Atmospheric Administration, 47p.

Dawson, R.J.; Dickson, M.E.; Nicholls, R.J.; Hall, J.W.; Walkden, M.J.A.; Stansby, P.K.; Mokrech, M.; Richards, J.; Zhou, J.; Milligan, J.; Jordan, A.; Pearson, S.; Rees, J.; Bates, P.D.; Koukoulas, S., and Watkinson, A.R., 2009. Integrated analysis of risks of coastal flooding and cliff erosion under scenarios of long term change. *Climatic Change,* 95(1–2), 249–288. doi:10.1007/s10584-008-9532-8

Enfield, D.B. and Allen, J.S., 1980. On the structure and dynamics of monthly mean sea-level anomalies along the Pacific coast of North and South America. *Journal of Physical Oceanography,* 10(4), 557–578. doi:10.1175/1520-0485(1980)010<0557:Otsado>2.0.Co;2

Erikson, L.H.; Hegermiller, C.A.; Barnard, P.L.; Ruggiero, P., and van Ormondt, M., 2015. Projected wave conditions in the Eastern North Pacific under the influence of two CMIP5 climate scenarios. *Ocean Modelling,* 96, Part 1, 171–185. doi:http://dx.doi.org/10.1016/j.ocemod.2015.07.004

Farnsworth, K.L. and Warrick, J.A., 2007. *Sources, Dispersal, and Fate of Fine Sediment Supplied to Coastal California*. U.S. Geological Survey, *Scientific Investigations Report 2007–5254*, 77p.

Flick, R.E., 1998. Comparison of California tides, storm surges, and mean sea level during the El Niño winters of 1982–83 and 1997–98. *Shore & Beach,* 66(3), 7–11.

Flick, R.E. 2016. California tides, sea level, and waves—Winter 2015–16. *Shore Beach,* 84(2), 25–30.

Flick, R.E. and Cayan, D.R., 1984. Extreme sea levels on the coast of California. *In:* Edge, B.L. (ed.), *Coastal Engineering 1984 Proceedings* (Houston, Texas), pp. 886–898.

Flint, L.E. and Flint, A.L., 2012. *Simulation of Climate Change in San Francisco Bay Basins, California: Case Studies in the Russian River Valley and Santa Cruz Mountains: U.S. Geological Survey Scientific Investigations Report 2012–5132*, 55p.

Griggs, G.B. and Paris, L., 1982. Flood control failure: San Lorenzo River, California. *Environmental Management,* 6(5), 407–419.

Guillén, J.; Bourrin, F.; Palanques, A.; De Madron, X.D.; Puig, P., and Buscail, R., 2006. Sediment dynamics during wet and dry storm events on the Têt inner shelf (SW Gulf of Lions). *Marine Geology,* 234(1), 129–142.

Guza, R.T. and Feddersen, F., 2012. Effect of wave frequency and directional spread on shoreline runup. *Geophysical Research Letters,* 39, L11607. doi:10.1029/2012gl051959

Hallegatte, S.; Green, C.; Nicholls, R.J., and Corfee-Morlot, J., 2013. Future flood losses in major coastal cities. *Nature Climate Change,* 3(9), 802–806. doi:10.1038/Nclimate1979

Heberger, M.; Cooley, H.; Herrera, P.; Gleick, P.H., and Moore, E., 2009. *The Impacts of Sea-Level Rise on the California Coast*. California Climate Change Center, *Report CEC-500-2009-024-F*, 115p.

Hinkel, J.; Lincke, D.; Vafeidis, A.T.; Perrette, M.; Nicholls, R.J.; Tol, R.S.J.; Marzeion, B.; Fettweis, X.; Ionescu, C., and Levermann, A., 2014. Coastal flood damage and adaptation costs under 21st century sea-level rise. *Proceedings of the National Academy of Sciences of the United States of America,* 111(9), 3292–3297. doi:10.1073/pnas.1222469111

IPCC (Intergovernmental Panel on Climate Change), 2013. *Climate Change 2013: The Physical Science Basis*. New York: Cambridge University Press, 1535p.

Jacobs, D.; Stein, E.D., and Longcore, T., 2010. *Classification of California Estuaries Based on Natural Closure Patterns: Templates for Restoration and Management*. Southern California Coastal Water Research Project, *Technical Report 619*, 50p.

Kang, L.; Ma, L., and Liu, Y., 2016. Evaluation of farmland losses from sea level rise and storm surges in the Pearl River Delta region under global climate change. *Journal of Geographical Sciences,* 26(4), 439–456. doi:10.1007/s11442-016-1278-z

Kates, R.W.; Colten, C.E.; Laska, S., and Leatherman, S.P., 2006. Reconstruction of New Orleans after Hurricane Katrina: A research perspective. *Proceedings of the National Academy of Sciences of the United States of America,* 103(40), 14653–14660. doi:10.1073/pnas.0605726103

Knauss, J.A., 1978. *Introduction to Physical Oceanography*. Englewood Cliffs, New Jersey: Prentice-Hall International, 338p.

Kniskern, T.A.; Warrick, J.A.; Farnsworth, K.L.; Wheatcroft, R.A., and Goni, M.A., 2011. Coherence of river and ocean conditions along the US West Coast during storms. *Continental Shelf Research,* 31(7–8), 789–805. doi:10.1016/j.csr.2011.01.012

Little, C.M.; Horton, R.M.; Kopp, R.E.; Oppenheimer, M.; Vecchi, G.A., and Villarini, G., 2015. Joint projections of US East Coast sea level and storm surge. *Nature Climate Change,* 5(12), 1114–1120. doi:10.1038/nclimate2801

Mawdsley, R.J. and Haigh, I.D., 2016. Spatial and temporal variability and long-term trends in skew surges globally. *Frontiers in Marine Science,* 3(29). doi:10.3389/fmars.2016.00029

McVan, D.C., 1997. *Model Study of the Confluence of San Juan Creek and Trabuco Creek, Orange County, California*. U.S. Army Corps of Engineers, *Technical Report CHL-97-25*, 201p.

Merkens, J.L.; Reimann, L.; Hinkel, J., and Vafeidis, A.T., 2016. Gridded population projections for the coastal zone under the Shared Socioeconomic Pathways. *Global and Planetary Change,* 145, 57–66. doi:10.1016/j.gloplacha.2016.08.009

Milly, P.C.D.; Wetherald, R.T.; Dunne, K., and Delworth, T.L., 2002. Increasing risk of great floods in a changing climate. *Nature,* 415(6871), 514–517.

Moore, L.J.; Benumof, B.T., and Griggs, G.B., 1999. Coastal erosion hazards in Santa Cruz and San Diego Counties, California. *Journal of Coastal Research,* Special Issue No. 28, pp. 121–139.

National Research Council, 2012. *Sea-Level Rise for the Coasts of California, Oregon, and Washington: Past, Present, and Future*. Washington, D.C.: National Academies Press, 201p.

Neumann, B.; Vafeidis, A.T.; Zimmermann, J., and Nicholls, R.J., 2015. Future coastal population growth and exposure to sea-level

rise and coastal flooding – a global assessment. *PLoS One,* 10(6), e0118571. doi:10.1371/journal.pone.0131375

NOAA (National Oceanic and Atmospheric Administration) (a). *National Data Buoy Center*. http://www.ndbc.noaa.gov/.

NOAA (b). *Tides and Currents*. https://tidesandcurrents.noaa.gov/.

OSHPD (California's Office of Statewide Health Planning and Development). *California Medical Service Study Areas (MSSA) Frontier, Rural and Urban Defined Areas*. https://www.oshpd.ca.gov/documents/HWDD/GIS/RuralMSSAv3.pdf.

Rahmstorf, S., 2007. A semi-empirical approach to projecting future sea-level rise. *Science,* 315(5810), 368–370. doi:10.1126/science.1135456

Ralph, F.M.; Neiman, P.J.; Wick, G.A.; Gutman, S.I.; Dettinger, M.D.; Cayan, D.R., and White, A.B., 2006. Flooding on California's Russian River: Role of atmospheric rivers. *Geophysical Research Letters,* 33(13). doi:10.1029/2006gl026689

Rotzoll, K. and Fletcher, C.H., 2013. Assessment of groundwater inundation as a consequence of sea-level rise. *Nature Climate Change,* 3(5), 477–481. doi:10.1038/nclimate1725

Ruggiero, P., 2013. Is the intensifying wave climate of the US Pacific Northwest increasing flooding and erosion risk faster than sea-level rise? *Journal of Waterway Port Coastal and Ocean Engineering,* 139(2), 88–97. doi:10.1061/(Asce)Ww.1943-5460.0000172

Ruggiero, P.; Komar, P.D.; McDougal, W.G.; Marra, J.J., and Beach, R.A., 2001. Wave runup, extreme water levels and the erosion of properties backing beaches. *Journal of Coastal Research,* 17(2), 407–419.

Scavia, D.; Field, J.C.; Boesch, D.F.; Buddemeier, R.W.; Burkett, V.; Cayan, D.R.; Fogarty, M.; Harwell, M.A.; Howarth, R.W.; Mason, C.; Reed, D.J.; Royer, T.C.; Sallenger, A.H., and Titus, J.G., 2002. Climate change impacts on US coastal and marine ecosystems. *Estuaries,* 25(2), 149–164. doi:10.1007/Bf02691304

Schwarz, K.M. and Orme, A.R., 2005. Opening and closure of a seasonal river mouth: The Malibu estuary–barrier–lagoon system, California. *Zeitschrift für Geomorphologie,* 141, S91–S109.

Serafin, K.A. and Ruggiero, P., 2014. Simulating extreme total water levels using a time-dependent, extreme value approach. *Journal of Geophysical Research: Oceans,* 119(9), 6305–6329. doi:10.1002/2014jc010093

Sloan, J.; Miller, J.R., and Lancaster, N., 2001. Response and recovery of the Eel River, California, and its tributaries to floods in 1955, 1964, and 1997. *Geomorphology,* 36(3), 129–154.

Sommerfield, C.K.; Drake, D.E., and Wheatcroft, R.A., 2002. Shelf record of climatic changes in flood magnitude and frequency, north-coastal California. *Geology,* 30(5), 395–398. doi:10.1130/0091-7613(2002)030<0395:srocci>2.0.co;2

Stockdon, H.F.; Holman, R.A.; Howd, P.A., and Sallenger, A.H., 2006. Empirical parameterization of setup, swash, and runup. *Coastal Engineering,* 53(7), 573–588. doi:10.1016/j.coastaleng.2005.12.005

Storlazzi, C.D. and Griggs, G.B., 2000. Influence of El Niño–Southern Oscillation (ENSO) events on the evolution of central California's shoreline. *Geological Society of America Bulletin,* 112(2), 236–249.

Storlazzi, C.D.; Willis, C.M., and Griggs, G.B., 2000. Comparative impacts of the 1982–83 and 1997–98 El Niño winters on the central California coast. *Journal of Coastal Research*, 16(4), 1022–1036.

The MathWorks, Inc., 2016. *MATLAB and Statistics Toolbox Release 2016b*. Natick, Massachusetts: The MathWorks, Inc.

U.S. Census Bureau. *State & County QuickFacts*. http://quickfacts.census.gov/qfd/states/06/06037.html.

U.S. Geological Survey (USGS). *National Water Information System: Web Interface*. http://waterdata.usgs.gov/nwis/sw.

Wahl, T.; Jain, S.; Bender, J.; Meyers, S.D., and Luther, M.E., 2015. Increasing risk of compound flooding from storm surge and rainfall for major US cities. *Nature Climate Change,* 5(12), 1093–1097.

Walter, L., 2015. *Ventura River Watershed Management Plan*. Ventura River Watershed Council. http://venturawatershed.org/wp-content/uploads/2011/12/VRWCPlan_Cover_TOC_Acknowledg.pdf.

Warrick, J.A.; Mertes, L.A.; Washburn, L., and Siegel, D.A., 2004. Dispersal forcing of southern California river plumes, based on field and remote sensing observations. *Geo-Marine Letters,* 24(1), 46–52.

Willis, C.M. and Griggs, G.B., 2003. Reductions in fluvial sediment discharge by coastal dams in California and implications for beach sustainability. *Journal of Geology,* 111(2), 167–182.

Wong, P.P.; Losada, I.J.; Gattuso, J.; Hinkel, J.; Khattabi, A.; McInnes, K.; Saito, Y., and Sallenger, A., 2014. Coastal systems and low-lying areas. *In:* Field, C.B.; Barros, V.R.; Dokken, D.J.; Mach, K.J.; Mastrandrea, M.D.; Bilir, T.E.; Chatterjee, M.; Ebi, K.L.; Estrada, Y.O.; Genova, R.C.; Girma, B.; Kissel, E.S.; Levy, A.N.; MacCracken, S.; Mastrandrea, P.R., and White L.L. (eds.), *Climate Change 2014: Impacts, Adaptation, and Vulnerability. Part A: Global and Sectoral Aspects*. Cambridge, U.K.: Cambridge University Press, pp. 361–409.

Young, I.R.; Zieger, S., and Babanin, A.V., 2011. Global trends in wind speed and wave height. *Science,* 332(6028), 451–455. doi:10.1126/science.1197219